American Mineralogist, Volume 95, pages 1027–1034, 2010

Low-temperature behavior of natural kalsilite with *P*31*c* symmetry: An in situ single-crystal X-ray diffraction study

G. DIEGO GATTA,[1,2,*] ROSS J. ANGEL,[3] AND MICHAEL A. CARPENTER[4]

[1]Dipartimento di Scienze della Terra, Università degli Studi di Milano, Via Botticelli 23, I-20133 Milano, Italy
[2]CNR-Istituto per la Dinamica dei Processi Ambientali, 20133 Milano, Italy
[3]Crystallography Laboratory, Department of Geosciences, Virginia Tech, Blacksburg, Virginia 24060, U.S.A.
[4]Department of Earth Sciences, University of Cambridge, Downing Street, Cambridge CB2 3EQ, U.K.

ABSTRACT

The low-temperature behavior of a natural kalsilite (ideal formula $KAlSiO_4$) with *P*31*c* symmetry has been investigated by in situ single-crystal diffraction. A series of intensity data collections and structural refinements have been performed at 298, 250, 200, 150, and 100 K on decreasing temperature, and 175, 225, and 275 K on increasing *T*. The variations of the unit-cell parameters of kalsilite as a function of *T* are continuous, and show no evidence of any phase transitions or thermo-elastic anomalies in this temperature range. An expansion is observed along [0001] with decreasing temperature. The axial and volume thermal expansion coefficients ($\alpha_j = l_j^{-1} \cdot \partial l_j / \partial T$, $\alpha_V = V^{-1} \cdot \partial V / \partial T$) between 298 and 100 K, calculated by weighted linear regression through the data points, are $\alpha_a = \alpha_b = 1.30(6) \cdot 10^{-5}$, $\alpha_c = -1.5(1) \cdot 10^{-5}$, $\alpha_V = 1.1(2) \cdot 10^{-5}$ K^{-1}. The main structural change on decreasing temperature is a cooperative anti-rotation of tetrahedra forming the six-membered rings lying parallel to (0001). This tetrahedral rotation is coupled with a change in the distances between the extra-framework cations and the framework O atoms. A small decrease in the tetrahedral tilts perpendicular to [0001] is responsible for the negative thermal expansion along [0001]; the implications of these mechanisms for thermal expansion in nephelines and kalsilites are discussed.

Keywords: Kalsilite, feldspathoids, low temperature, single-crystal X-ray diffraction, thermal expansion

INTRODUCTION

Kalsilite (ideal formula $KAlSiO_4$) is a framework silicate belonging to the "feldspathoid group." Kalsilite occurs mainly in K-rich and silica-undersaturated volcanic rocks, probably as a result of the breakdown of silica-rich leucite in alkalic ultramafic rocks, and is usually associated with olivine, melilite, clinopyroxene, phlogopite, nepheline, and leucite. Kalsilite also occurs in metamorphic rocks.

The tetrahedral framework of kalsilite is isotypic (or homeotypic) with tridymite and has topological symmetry $P6_3/mmc$, whereas the topochemical symmetry of kalsilite is $P6_3mc$ as a result of Al/Si ordering within the tetrahedra (Gottardi 1979). The tetrahedral framework consists of (0001) sheets of (ordered) AlO_4 and SiO_4 tetrahedra forming six-membered rings (hereafter 6mR), pointing alternately up (U) and down (D) [i.e., 6mR// (0001): UDUDUD, Fig. 1]. The sheets are stacked along the **c**-axis and joined through the apical O1 atoms, which formally occupy special positions on the threefold axis. However, Perrotta and Smith (1965) found that this bridging oxygen is displaced by ~0.25 Å from the threefold axis, giving Al-O-Si bond angles <180°. The tetrahedral rings are also di-trigonally distorted by rotation of the tetrahedra around [0001], with the sense of rotation reversed between adjacent (0001) sheets. A second set of 6-membered rings of tetrahedra occur perpendicular to (0001) [Fig. 1, hereafter 6mR⊥(0001)].

Cellai et al. (1997) reported the crystal structure of essentially Na-free metamorphic kalsilite (i.e., K/Na molar ratio ~350). The authors showed that the structure has *P*31*c* symmetry. The crystals were ubiquitously twinned across (0001) so that *hkl* reflections of the first individual were superimposed on the $hk\bar{l}$ reflections from its twin. The structural model of *P*31*c* kalsilite shows an identical configuration of the tetrahedral sheets with those of the $P6_3$ structure. However, the sheets are stacked in an eclipsed manner, with the same rotation of the 6mR//(0001) in succeeding sheets (Cellai et al. 1997) (Fig. 1). In the structural model described in space group *P*31*c*, the bridging oxygen between the sheets lies on the triad axis, giving an unusual Si-O-Al angle of 180°. The authors reported no experimental evidence for splitting of the bridging oxygen off the threefold axis, but a strong anisotropy of the thermal ellipsoid of the apical oxygen was observed, which is probably due to a static or dynamic disorder of the oxygen position, and the apparent inter-sheet Al-O-Si bond angle 180° is just an artifact of averaging.

A significant number of experiments has been devoted to the thermo-elastic behavior, high-temperature structural modification and phase-stability of kalsilite (Tuttle and Smith 1958; Sahama 1962a, 1962b; Henderson and Roux 1976, 1977; Dollase and Freeborn 1977; Gregorkiewitz and Schäfer 1980; Andou and Kawahara 1982, 1984; Henderson and Taylor 1982, 1988; Abbott 1984; Merlino 1984; Kawahara et al. 1987; Hovis and Roux 1993; Xu and Veblen 1996; Capobianco and Carpenter 1989; Carpenter and Cellai 1996; Cellai et al. 1999; Hovis and

* E-mail: diego.gatta@unimi.it

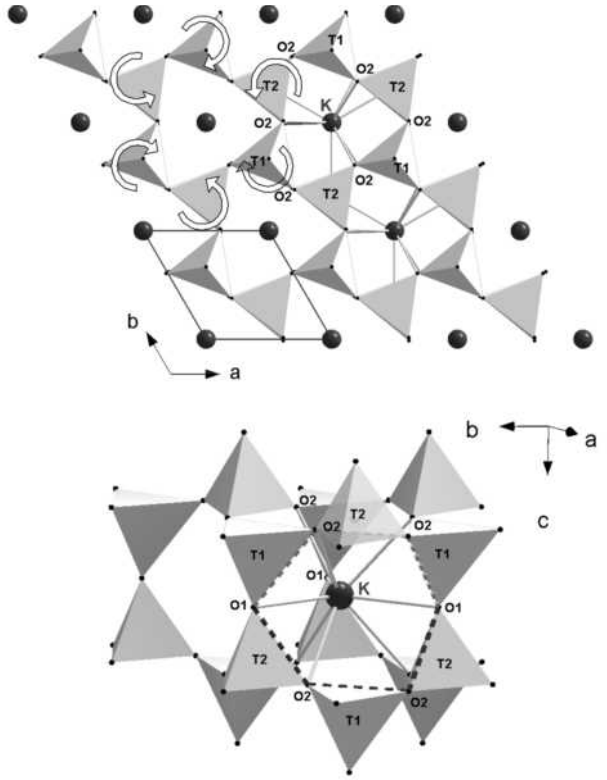

FIGURE 1. (**top**) A single (0001) tetrahedral sheet of kalsilite. The arrows indicate the rotations of tetrahedra on decreasing temperature, which increase the ditrigonal distortion of the 6mR//(0001). (**bottom**) Clinographic view of the three-dimensional framework of *P*31*c* kalsilite. The dark-gray and light-gray dotted lines outline the 6mR⊥(0001) and indicate the O1-O2-O2′-O1′$_s$ and O1-O2-O2′-O1′$_l$ torsion angles, respectively (Table 3).

Crelling 2000; Hovis et al. 1999, 2003, 2006, 2009). Hovis and Roux (1993, 1999) investigated the nepheline-kalsilite crystalline solutions, showing three room-temperature phases along the join, namely (with increasing K content) nepheline, tetrakalsilite, and kalsilite. Merlino (1984) and Hovis and Roux (1993, 1999) highlighted that even though these three compounds are isotypic stuffed derivatives of tridymite, they differ in the framework configuration and in the number, nature and bonding-scheme of extra-framework alkali sites. Several structures of kalsilite stable at high temperature have been reported, giving a complex picture of the HT phase-stability of kalsilite, which appears to be strongly controlled by the Na content. Carpenter and Cellai (1996) and Cellai et al. (1999) showed that the metamorphic *P*31*c* "pure" kalsilite experiences an irreversible phase transition to *P*6$_3$ upon heating, which is complete at ~500 °C. The high-temperature framework configuration is achieved by tetrahedral rotation such that successive (0001) sheets undergo opposite-sense rotations. The authors highlighted how the refined high-temperature structure shows strong similarities with that of the volcanic kalsilite (i.e., with *P*6$_3$ symmetry at room conditions, Perrotta and Smith 1965). In the high-temperature *P*6$_3$ structure of metamorphic kalsilite, the refined thermal ellipsoid of both apical and basal O atoms are significantly anisotropic, even though the apical oxygen lies on the triad axis and not off-axis, as observed in volcanic *P*6$_3$ kalsilite. The authors suggested that the more pronounced positional disorder in volcanic kalsilite might be due to the presence of sodium, which was almost absent in the metamorphic kalsilite used by Cellai et al. (1997, 1999).

Despite the many experiments devoted to the high-temperature behavior of kalsilite, no structural data have been reported for kalsilite at low temperature. At low temperatures, the atomic thermal motion is significantly reduced, and the main deformation mechanisms (e.g., polyhedral rotation and tilting) can be followed more clearly as they are less obscured by the thermal contribution to the atomic displacement parameters. In addition, at low *T*, phenomena like extra-framework cation disorder or Al/Si-reordering are unlikely. On this basis, the aim of this study was the investigation of the thermo-elastic behavior and the low-temperature structural evolution of kalsilite by means of in situ single-crystal X-ray diffraction to determine if it is the same as that of nepheline (Angel et al. 2008) and to determine the structural mechanism behind the negative thermal expansion of the *c* axis (Hovis et al. 2003).

STARTING MATERIAL AND EXPERIMENTAL METHODS

Measurements were performed on crystals of metamorphic kalsilite from the sample studied by Carpenter and Cellai (1996) and Cellai et al. (1997, 1999). The kalsilite crystals were collected from a granulite facies gneiss from the Punalur district in Kerala, southern India (provided by M. Santosh). The Punalur assemblages consists of kalsilite, leucite, hibonite, spinel, corundum, titanite, perovskite, Ti-bearing phlogopite, and potassium feldspar. Peak metamorphic conditions of the Punalur gneiss have been estimated as 700–800 °C and 3.5–6.5 kbars (Sandiford and Santosh 1991). The kalsilite from Punalur is essentially end-member $KAlSiO_4$, with a K/Na molar ratio of ~350 (Capobianco and Carpenter 1989; Sandiford and Santosh 1991; Cellai et al. 1997, 1999).

For the low-*T* diffraction experiment, we selected two series of crystals of kalsilite that were annealed: (1) at 500 °C for 4 days and (2) at 900 °C for 1 h by Cellai et al. (1999). Immediately after annealing in 1995 both samples were shown to display *P*6$_3$ symmetry at room temperature. Surprisingly, all of the more than 30 crystals that we checked in 2009 by single-crystal X-ray diffraction showed *P*31*c* symmetry. In other words, the *P*31*c*-to-*P*6$_3$ phase transition upon heating reported as "irreversible" by Cellai et al. (1997) is actually "reversible," on the time scale of a decade. We therefore performed our low-*T* experiment with a crystal of *P*31*c* kalsilite.

Single-crystal diffraction data were first collected at 298 K using an Oxford Diffraction Gemini diffractometer equipped with a Sapphire-III CCD detector and graphite monochromated Mo*K*α radiation (Enhance X-ray optics). The diffractometer was operated at 50 kV and 40 mA. A combination of ω and φ scans was used to maximize the reciprocal space coverage and redundancy, with a fixed exposure time per frame (5 s/frame) and a crystal-detector distance of 50 mm (Table 1). The low-temperature data sets were all collected in a single excursion from room temperature to 100 K and back, with data sets collected at 250, 200, 150, and 100 K on cooling and at 175, 225, and 275 K on warming (Table 1). A Cryojet open-flow nitrogen gas system with a temperature stability of better than 0.2 K and absolute uncertainty in temperature at the crystal position of <2 K was used. Each data collection took ~3 h, and temperature ramps between data collections took 15–20 min.

The diffraction patterns at all temperatures confirmed that the lattice remained metrically trigonal, with reflection conditions consistent with space group *P*31*c* (Cellai et al. 1997). No super-lattice reflections (Smith and Sahama 1957; Perrotta and Smith 1965; Carpenter and Cellai 1996; Xu and Veblen 1996) were observed. No evidence of any phase transition was found within the *T*-range investigated. Data reduction (CrysAlis, Oxford Diffraction 2007) included an analytical absorption correction by Gaussian integration based upon the physical description of the crystal.

All structure refinements were performed using the SHELX-97 software (Sheldrick 2008), starting from the atomic coordinates of Cellai et al. (1997) in space group *P*31*c* and Cellai et al. (1999) in space group *P*6$_3$. Floating origin restraints, necessary for the non-centrosymmetric space groups, were automatically

TABLE 1. Details of data collections and refinements of kalsilite at different temperatures

T (K)	298	250	200	150	100	175	225	275
Crystal size (μm × μm × μm)	240 × 190 × 120	240 × 190 × 120	240 × 190 × 120	240 × 190 × 120	240 × 190 × 120	240 × 190 × 120	240 × 190 × 120	240 × 190 × 120
a (Å)	5.1665(6)	5.1627(4)	5.1588(4)	5.1560(4)	5.1531(4)	5.1589(4)	5.1627(4)	5.1652(5)
c (Å)	8.7248(13)	8.7352(10)	8.7383(10)	8.7450(9)	8.7523(8)	8.7438(9)	8.7392(10)	8.7326(11)
V (Å^3)	201.69(6)	201.63(5)	201.40(5)	201.33(5)	201.27(6)	201.35(5)	201.72(5)	201.76(6)
Space group	*P*31*c*	*P*31*c*	*P*31*c*	*P*31*c*	*P*31*c*	*P*31*c*	*P*31*c*	*P*31*c*
Radiation	Mo*K*α	Mo*K*α	Mo*K*α	Mo*K*α	Mo*K*α	Mo*K*α	Mo*K*α	Mo*K*α
Detector type	CCD	CCD	CCD	CCD	CCD	CCD	CCD	CCD
Crystal-detector distance (mm)	50	50	50	50	50	50	50	50
Scan type	ω/ϕ	ω/ϕ	ω/ϕ	ω/ϕ	ω/ϕ	ω/ϕ	ω/ϕ	ω/ϕ
Exposure time (s)	5	5	5	5	5	5	5	5
2θ max (°)	80.27	82.04	82.11	82.16	82.21	82.11	82.04	82.00
	$-7 \le h \le 9$	$-7 \le h \le 9$	$-7 \le h \le 9$	$-7 \le h \le 9$	$-7 \le h \le 9$	$-7 \le h \le 9$	$-7 \le h \le 9$	$-7 \le h \le 9$
	$-9 \le k \le 7$	$-9 \le k \le 8$	$-9 \le k \le 8$	$-9 \le k \le 8$	$-9 \le k \le 8$	$-9 \le k \le 8$	$-9 \le k \le 8$	$-9 \le k \le 8$
	$-15 \le l \le 12$	$-16 \le l \le 12$	$-16 \le l \le 12$	$-16 \le l \le 12$	$-16 \le l \le 12$	$-16 \le l \le 12$	$-16 \le l \le 12$	$-16 \le l \le 12$
Coverage	>99.5%	>99.5%	>99.5%	>99.5%	>99.5%	>99.5%	>99.5%	>99.5%
Redundancy	3.5	3.5	3.5	3.5	3.5	3.5	3.5	3.5
No. measured reflections	4095	4170	4158	4148	4113	4141	4146	4179
No. unique reflections	797	825	822	817	815	821	822	824
No. unique reflections with $F_o > 4\sigma(F_o)$	592	617	626	622	634	624	613	613
No. refined parameters	24	24	24	24	24	24	24	24
R_{int}	0.0518	0.0512	0.0529	0.0543	0.0562	0.0553	0.0554	0.0516
$R_1(F)$ with $F_o > 4\sigma(F_o)$	0.0340	0.0338	0.0326	0.0335	0.0332	0.0334	0.0339	0.0357
$wR_2(F^2)$	0.0575	0.0557	0.0544	0.0603	0.0624	0.0597	0.0588	0.0582
GooF	1.541	1.505	1.449	1.561	1.470	1.590	1.506	1.535
Residuals (e^-/Å^3)	−0.40/+0.47	−0.42/+0.48	−0.32/+0.48	−0.39/+0.49	−0.34/+0.56	−0.45/+0.48	−0.34/+0.51	−0.44/+0.54

Notes: $R_{int} = \Sigma|F^2_{obs} - F^2_{obs}(mean)|/\Sigma[F^2_{obs}]$; $R_1 = \Sigma(||F_{obs}| - |F_{calc}||)/\Sigma|F_{obs}|$; $wR_2 = \{\Sigma[w(F^2_{obs} - F^2_{calc})^2]/\Sigma[w(F^2_{obs})^2]\}^{0.5}$, $w = 1/[\sigma^2(F^2_{obs}) + (0.01 \cdot P)^2]$, $P = [\mathrm{Max}(F^2_{obs}, 0) + 2 \cdot F^2_{calc}]/3$. The Flack parameter (Sheldrick 1997) refined at 298 K is $x = 0.51(8)$.

generated by SHELX-97. Neutral atomic scattering factors for K, Si, Al, and O were taken from the *International Tables for Crystallography* (Wilson and Prince 1999). The structural refinements proved, unambiguously, that within the *T*-range investigated kalsilite maintains *P*31*c* symmetry. The crystal of kalsilite used for the low-*T* experiment was twinned by reticular merohedry with an (0001) twin plane, as previously observed for the Punalur kasilite (Cellai et al. 1997). The refined volumes of the two twin components approached 50% each (Table 1). The refined occupancy factor of the K-site showed a small, but significant, potassium deficiency (Table 2). The intra-tetrahedral bond distances suggested a fully (or highly) ordered Si/Al-distribution in the tetrahedral framework, with the O1 bridging oxygen lying on the triad axis (Table 2). A mixed scattering curve based on mixed occupancies of the T1 and T2 tetrahedral sites by Al and Si did not significantly improve the figures of merit of the refinement, and all final refinements were performed with scattering factors corresponding to a fully ordered model for tetrahedral occupancies. Correction for secondary isotropic extinction was not necessary. Convergence was rapidly achieved after a few least-square cycles of refinement and the variance-covariance matrix did not show any significant correlation between the refined parameters at any given temperature. At the end of refinements, the residual electron density in the difference-Fourier maps was between approximately ±0.5 e$^-$/Å^3, with agreement factors $R_1(F) < 0.035$ and (No. observations/No. refined parameter) > 25 at all temperatures (Table 1).

RESULTS AND DISCUSSION

The variation of the unit-cell parameters of kalsilite as a function of *T* are shown in Figure 2. Each trend is continuous, showing no phase transition or thermo-elastic anomaly within the *T*-range investigated, but the *c*-axis displays negative thermal expansion as it does at higher temperatures (Hovis et al. 2003). The structural cause of the negative thermal expansion of the *c*-axis will be described below. The unit-cell parameters measured on increasing temperature are parallel, but offset from, the trend observed on decreasing temperature (Fig. 2). The axial and volume thermal expansion coefficients ($\alpha_j = l_j^{-1} \cdot \partial l_j / \partial T$, $\alpha_V = V^{-1} \cdot \partial V / \partial T$) between 298 and 100 K were calculated by weighted linear regression using only the data collected on decreasing temperature, yielding $\alpha_a = \alpha_b = 1.30(6) \cdot 10^{-5}$, $\alpha_c = -1.5(1) \cdot 10^{-5}$, $\alpha_V = 1.1(2) \cdot 10^{-5}$ K^{-1}. As expected, the low-temperature coefficient of linear volume thermal expansion is smaller than the value of $\alpha_V \approx 3.43 \cdot 10^{-5}$ K^{-1} measured for a Na-poor kalsilite (X_{Ks} = 0.983) between 298 and 1170 K (Hovis et al. 2003). The volume thermal expansion of kalsilite is also significantly less than that of nepheline. This has been attributed to the kalsilite framework being expanded relative to that of nepheline as a consequence of the presence of a larger K extra-framework cation in place of the Na+K content of nephelines (Hovis et al. 2003).

The refined T-O bond distances show a marginal increase at low temperatures (Table 3) that can be explained as the result of a combination of significant thermal vibrations (probably librations of the tetrahedra) and/or static rotations and tilts of the tetrahedra, which are reflected in the large refined values of some atomic displacement parameters. After correction for "rigid body motion" effects, following the protocol described by Downs et al. (1992) and Downs (2000), the differences in the intra-tetrahedral bond distances at 300 and 100 K are <0.003 Å (Table 3). Therefore, as expected for the temperatures involved, there is no evidence for any redistribution of Al and Si within the structure during the experimental measurements.

The structures of nepheline and kalsilite share the same framework topology, with 6mR of tetrahedra that form the channels within which the K (kalsilite) and Na and K (nepheline) are located. These rings form (0001) sheets of tetrahedra that undergo two basic types of deformation in response to changes in temperature, pressure and the chemical content of the extra-framework channels: cooperative rotation around [0001], which

TABLE 2. Refined positional and thermal displacement parameters (Å^2) of kalsilite at different temperatures

Site (Wyck.)	*x*	*y*	*z*	*s.o.f.*	U_{11}	U_{22}	U_{33}	U_{23}	U_{13}	U_{12}	U_{eq}
298 K											
K1 (2*a*)	0	0	0.2532(6)	0.985(3)	0.0186(2)	0.0186(2)	0.0213(4)	0	0	0.0093(1)	0.0195(2)
T1 (2*b*)	1/3	2/3	0.0620(1)	1	0.0108(7)	0.0108(7)	0.0143(10)	0	0	0.0054(4)	0.0120(5)
T2 (2*b*)	1/3	2/3	0.44379(7)	1	0.0085(5)	0.0085(5)	0.0091(7)	0	0	0.0042(3)	0.0087(4)
O1 (2*b*)	1/3	2/3	0.2591(5)	1	0.0393(8)	0.0393(8)	0.0124(11)	0	0	0.0196(4)	0.0303(5)
O2 (6*c*)	0.6164(5)	0.0132(8)	1.0025(12)	1	0.0100(11)	0.0138(8)	0.0312(8)	0.0045(9)	0.0024(22)	0.0034(11)	0.0195(3)
250 K											
K1 (2*a*)	0	0	0.2536(6)	0.982(2)	0.0161(2)	0.0161(2)	0.0183(3)	0	0	0.00804(9)	0.0168(1)
T1 (2*b*)	1/3	2/3	0.0622(1)	1	0.0109(6)	0.0109(6)	0.0119(10)	0	0	0.0054(3)	0.0112(5)
T2 (2*b*)	1/3	2/3	0.44419(7)	1	0.0073(5)	0.0073(5)	0.0089(7)	0	0	0.0036(2)	0.0078(3)
O1 (2*b*)	1/3	2/3	0.2595(5)	1	0.0359(7)	0.0359(7)	0.0113(11)	0	0	0.0179(4)	0.0277(5)
O2 (6*c*)	0.6179(4)	0.0141(8)	1.0041(10)	1	0.0086(10)	0.0117(8)	0.0279(6)	0.0034(9)	0.0016(19)	0.0019(9)	0.0175(3)
200 K											
K1 (2*a*)	0	0	0.2526(5)	0.987(3)	0.0136(2)	0.0136(2)	0.0152(3)	0	0	0.00682(8)	0.0142(1)
T1 (2*b*)	1/3	2/3	0.0619(1)	1	0.0080(7)	0.0080(7)	0.0119(9)	0	0	0.0040(3)	0.0093(4)
T2 (2*b*)	1/3	2/3	0.44383(5)	1	0.0071(5)	0.0071(5)	0.0071(7)	0	0	0.0036(3)	0.0071(3)
O1 (2*b*)	1/3	2/3	0.2590(5)	1	0.0320(6)	0.0320(6)	0.0103(10)	0	0	0.0160(3)	0.0248(4)
O2 (6*c*)	0.6196(4)	0.0146(7)	1.0042(10)	1	0.0073(9)	0.0101(7)	0.0234(6)	0.0028(9)	0.0016(17)	0.0018(9)	0.0148(3)
150 K											
K1 (2*a*)	0	0	0.2532(5)	0.983(3)	0.0113(2)	0.0113(2)	0.0125(3)	0	0	0.00566(8)	0.0117(1)
T1 (2*b*)	1/3	2/3	0.0619(1)	1	0.0091(6)	0.0091(6)	0.0106(10)	0	0	0.0046(3)	0.0096(4)
T2 (2*b*)	1/3	2/3	0.44386(6)	1	0.0057(5)	0.0057(5)	0.0063(7)	0	0	0.0028(2)	0.0059(3)
O1 (2*b*)	1/3	2/3	0.2589(5)	1	0.0289(7)	0.0289(7)	0.0096(10)	0	0	0.0144(3)	0.0225(5)
O2 (6*c*)	0.6204(5)	0.0140(7)	1.0036(10)	1	0.0063(9)	0.0099(8)	0.0204(6)	0.0015(8)	0.0020(18)	0.0010(9)	0.0136(3)
100 K											
K1 (2*a*)	0	0	0.2529(5)	0.984(3)	0.0089(1)	0.0089(1)	0.0097(2)	0	0	0.00443(8)	0.0091(1)
T1 (2*b*)	1/3	2/3	0.0618(1)	1	0.0069(6)	0.0069(6)	0.0096(9)	0	0	0.0034(3)	0.0078(4)
T2 (2*b*)	1/3	2/3	0.44388(6)	1	0.0054(5)	0.0054(5)	0.0049(7)	0	0	0.0027(3)	0.0052(3)
O1 (2*b*)	1/3	2/3	0.2588(5)	1	0.0239(6)	0.0239(6)	0.0078(9)	0	0	0.0119(3)	0.0185(4)
O2 (6*c*)	0.6215(4)	0.0147(7)	1.0041(10)	1	0.0054(9)	0.0070(7)	0.0180(5)	0.0007(8)	0.0003(17)	0.0009(8)	0.0111(3)
175 K											
K1 (2*a*)	0	0	0.2532(5)	0.980(3)	0.0124(2)	0.0124(2)	0.0142(3)	0	0	0.00621(9)	0.0130(1)
T1 (2*b*)	1/3	2/3	0.0619(1)	1	0.0093(7)	0.0093(7)	0.0115(9)	0	0	0.0047(3)	0.0101(5)
T2 (2*b*)	1/3	2/3	0.44386(6)	1	0.0064(5)	0.0064(5)	0.0064(7)	0	0	0.0032(2)	0.0064(3)
O1 (2*b*)	1/3	2/3	0.2591(5)	1	0.0302(7)	0.0302(7)	0.0106(11)	0	0	0.0151(3)	0.0237(5)
O2 (6*c*)	0.6196(4)	0.0137(8)	1.0032(10)	1	0.0066(9)	0.0104(8)	0.0223(6)	0.0019(8)	0.0001(19)	0.0012(9)	0.0145(3)
225 K											
K1 (2*a*)	0	0	0.2530(5)	0.985(3)	0.0149(2)	0.0149(2)	0.0164(3)	0	0	0.00744(9)	0.0154(1)
T1 (2*b*)	1/3	2/3	0.0619(1)	1	0.0074(7)	0.0074(7)	0.0131(9)	0	0	0.0037(4)	0.0093(5)
T2 (2*b*)	1/3	2/3	0.44384(7)	1	0.0089(6)	0.0089(6)	0.0065(6)	0	0	0.0044(3)	0.0081(4)
O1 (2*b*)	1/3	2/3	0.2590(5)	1	0.0341(7)	0.0341(7)	0.0104(10)	0	0	0.0170(5)	0.0262(5)
O2 (6*c*)	0.6190(5)	0.0146(7)	1.0043(10)	1	0.0074(9)	0.0108(7)	0.0252(6)	0.0018(9)	0.0012(19)	0.0013(9)	0.0159(3)
275 K											
K1 (2*a*)	0	0	0.2532(6)	0.986(3)	0.0175(2)	0.0175(2)	0.0202(3)	0	0	0.0088(1)	0.0184(2)
T1 (2*b*)	1/3	2/3	0.0620(1)	1	0.0110(7)	0.0110(7)	0.0137(10)	0	0	0.0055(3)	0.0119(5)
T2 (2*b*)	1/3	2/3	0.44378(6)	1	0.0080(5)	0.0080(5)	0.0086(7)	0	0	0.0040(2)	0.0082(3)
O1 (2*b*)	1/3	2/3	0.2591(5)	1	0.0386(8)	0.0386(8)	0.0115(11)	0	0	0.0193(4)	0.0295(5)
O2 (6*c*)	0.6173(5)	0.0138(8)	1.0036(11)	1	0.0087(10)	0.0131(8)	0.0287(7)	0.0036(9)	0.0001(20)	0.0018(10)	0.0184(3)

Notes: The anisotropic displacement factor exponent takes the form: $-2\pi^2[(ha^*)^2U_{11} + ... + 2hka^*b^*U_{12}]$. U_{eq} is defined as one third of the trace of the orthogonalized U_{ij} tensor. For the T1 and T2 sites, the neutral scattering curves of aluminum and silicon, respectively, were used.

leads to a reduction in the diameter of the extra-framework channels, and a cooperative tilting of the tetrahedra about an axis perpendicular to [0001]. Because consecutive (0001) sheets of tetrahedra are only linked through the apical O atoms of the tetrahedra, the rotations of the tetrahedra in consecutive (0001) sheets can be independent of one another if the T-O-T bond angles through these O atoms are almost straight (as in kalsilite). This allows the complex polymorphism and polytypism observed in kalsilite but not in nepheline (Merlino 1984; Kawahara et al. 1987; Hovis and Roux 1993; Xu and Veblen 1996; Capobianco and Carpenter 1989; Carpenter and Cellai 1996; Cellai et al. 1999; Hovis and Crelling 2000; Hovis et al. 1999, 2003, 2006, 2009). In the *P*31*c* kalsilite described here, all of the 6mRs in all of the sheets are distorted in the same sense and by the same amount. As a consequence, the framework contains only two symmetrically distinct tetrahedra, T1 and T2 (Table 2; Fig. 1), which alternate throughout the framework.

Within the average structure of *P*31*c* kalsilite, the T1 and T2 sites and the bridging oxygen O1 shared between them lie on the triad axis at $x = 1/3$, $y = 2/3$, making the T1-O1-T2 linkage linear. As a consequence, the T1 and the T2 tetrahedra are only allowed, on average, to rotate around [0001], and cannot tilt (as this would require either internal deformation of the O1-T-O2 angles or movement of the atoms from the triad axis). The T1 and T2 tetrahedra in nepheline are constrained in the same way (Angel et al. 2008). The greatest change to the average structure of kalsilite on decreasing temperature is the cooperative anti-rotation of all tetrahedra around [0001] so as to increase the distortion of the 6mR rings parallel to (0001), as shown in Figure 1. The *z*-coordinate of the O2 atom, which links the tetrahedra into these 6mR rings, does not change with temperature. Thus, there is no change in the O2-O1-O2 or O2-O2-O1 angles with *T* (Table 3; Figs. 1 and 3), but the two symmetrically distinct torsion angles O1-O2-O2′-$O1'_s$ and O1-O2-O2′-$O1'_t$ of the 6mR⊥(0001) (Table 3; Fig. 1) increase with decreasing *T* purely as a consequence of the tetrahedral rotations (Table 3; Fig. 3).

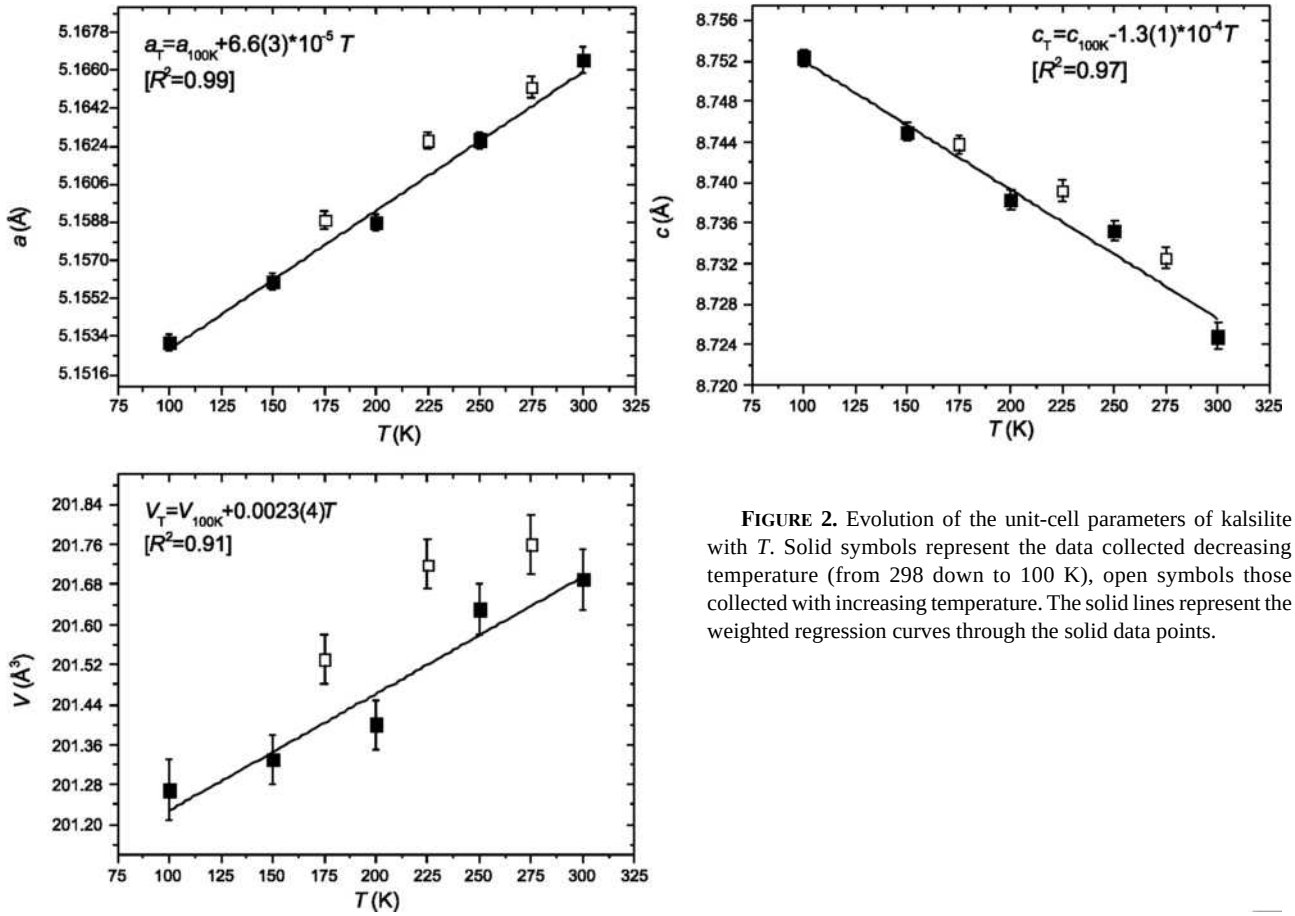

FIGURE 2. Evolution of the unit-cell parameters of kalsilite with *T*. Solid symbols represent the data collected decreasing temperature (from 298 down to 100 K), open symbols those collected with increasing temperature. The solid lines represent the weighted regression curves through the solid data points.

TABLE 3. Bond distances (Å) and angles (°) in the kalsilite structure at different temperatures

T (K)	298	250	200	150	100	175	225	275
K-O2	2.966(7)	2.965(7)	2.953(6)	2.957(7)	2.950(6)	2.961(6)	2.958(7)	2.967(7)
K-O2′	2.975(7)	2.971(7)	2.972(6)	2.962(7)	2.965(7)	2.962(6)	2.974(7)	2.972(7)
K-O1	2.9833(4)	2.9811(3)	2.9790(3)	2.9772(3)	2.9756(3)	2.9789(3)	2.9812(3)	2.9826(3)
T1-O1	1.720(4)	1.723(4)	1.722(4)	1.723(4)	1.724(4)	1.724(4)	1.723(4)	1.721(4)
	1.7357*				1.7330*			
T1-O2 (×3)	1.731(2)	1.732(2)	1.734(2)	1.734(2)	1.736(2)	1.734(2)	1.734(2)	1.731(2)
	1.7374*				1.7389*			
O1-T1-O2 (×3)	107.4(4)	107.1(3)	106.9(3)	107.1(3)	106.9(3)	107.2(3)	106.9(3)	107.1(3)
O2-T1-O2 (×3)	111.4(4)	111.8(3)	111.9(3)	111.8(3)	111.9(3)	111.6(3)	111.9(3)	111.7(3)
T2-O1	1.611(4)	1.613(4)	1.615(4)	1.617(4)	1.620(4)	1.616(4)	1.615(4)	1.613(4)
	1.6313*				1.6321*			
T2-O2 (×3)	1.623(2)	1.624(2)	1.625(2)	1.627(2)	1.627(2)	1.627(2)	1.625(2)	1.625(2)
	1.6333*				1.6320*			
O1-T2-O2 (×3)	108.4(4)	108.8(3)	108.9(3)	108.7(3)	108.9(3)	108.6(3)	109.0(3)	108.8(4)
O2-T2-O2 (×3)	110.5(4)	110.1(3)	110.0(3)	110.2(3)	110.0(3)	110.3(3)	110.0(3)	110.2(3)
O2-O2-O2s [6mR//(0001)]	78.3(1)	77.9(1)	77.5(1)	77.0(1)	75.8(1)	77.3(1)	77.6(1)	78.1(1)
O2-O2-O2l [6mR//(0001)]	161.7(2)	162.1(2)	162.61(1)	162.9(2)	163.2(1)	162.7(2)	162.3(1)	161.9(2)
O2-O1-O2 [6mR⊥(0001)]	107.6(2)	107.7(1)	107.6(1)	107.6(1)	107.7(1)	107.6(1)	107.7(1)	107.7(1)
O2-O2-O1	125.5(1)	125.6(1)	125.7(1)	125.5(1)	125.6(1)	125.5(1)	125.7(1)	125.6(1)
O1-O2-O2′-O1′$_s$	42.9(4)	42.9(3)	43.3(3)	43.7(3)	43.8(3)	43.6(3)	43.1(3)	42.8(4)
O1-O2-O2′-O1′$_l$	43.5(4)	44.0(3)	44.6(3)	44.8(3)	45.2(3)	44.5(3)	44.4(3)	43.9(4)

Note: The torsion angles O1-O2-O2′-O1′$_s$ and O1-O2-O2′-O1′$_l$ are defined according to Klyne and Prelog (1960).
* Bond distances corrected for "rigid body motions" effect (Downs 2000).

However, the large values of the thermal displacement parameter U_{11} for the O1 oxygen and U_{33} for the O2 oxygen (Table 2), indicate that this simple picture of the *P*31*c* kalsilite structure responding to temperature changes by simple tetrahedral rotation is not a complete picture of its local structure. The large values for the U_{11} displacement parameter of the O1 oxygen suggests static or dynamic displacements from the triad at $x = 1/3$, $y = 2/3$. A significant shift of O1 off the triad axis (1/3, 2/3, *z*) to a general position (*x*, *y*, *z*), with a formal average occupancy of 1/3, was observed in the $P6_3$ volcanic kalsilite (Perrotta and Smith 1965)

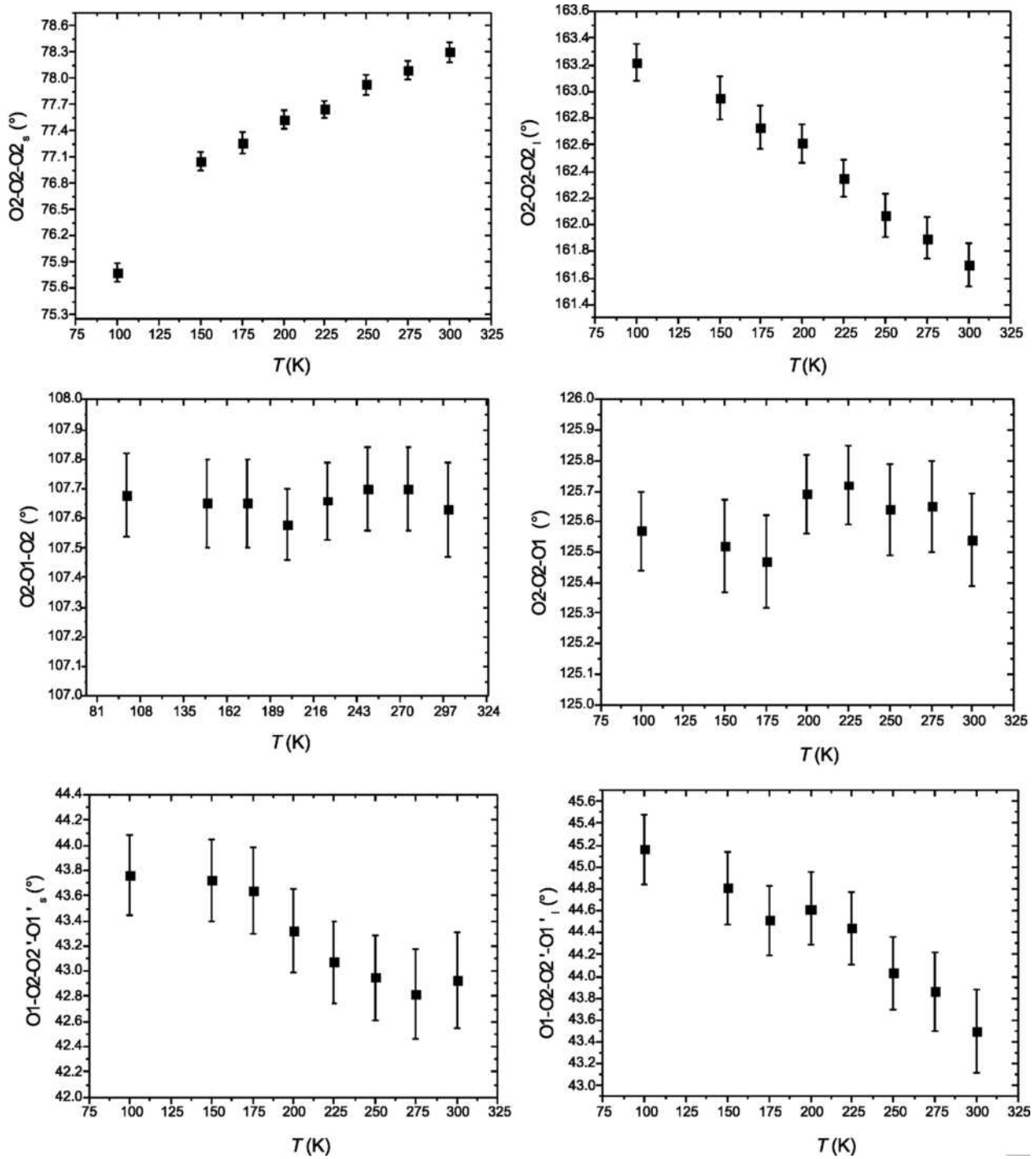

FIGURE 3. Evolution of the O-O-O angles with temperature. The tetrahedral rotation around [0001] is measured by changes in O2-O2-$O2_s$ and O2-O2-$O2_l$. These rotations contribute to very small changes in O2-O1-O2 and O2-O2-O1 angles in the 6mR⊥(0001). The O1-O2-O2′-$O1'_s$ and O1-O2-O2′-$O1'_l$ are torsion angles in the 6mR⊥(0001), as defined in Table 3 and Figure 1.

and in the isotypic nepheline (Gatta et al. 2007; Angel et al. 2008 and references therein), leading to a T-O-T angle significantly smaller than 180° and the implication that the tetrahedra are tilted. In our *P*31*c* kalsilite the effect is not so large, and in our refinements it was not possible to refine a split-site model for the O1 position. Therefore, the O1-site is formally located at (1/3, 2/3, *z*), but the significantly anisotropic thermal displacement ellipsoid (Fig. 4) indicates an average over a true local structure with T1-O1-T2 angles <180°. If one takes normal Al-O and Si-O bond lengths of around 1.73 and 1.62 Å, respectively, one can estimate from the T1-T2 distance that the true local value of the T1-O1-T2 angle is ~168° at room temperature, significantly greater than the T1-O1-T2 angle in ordered nepheline (~151°) at the same temperature (Angel et al. 2008).

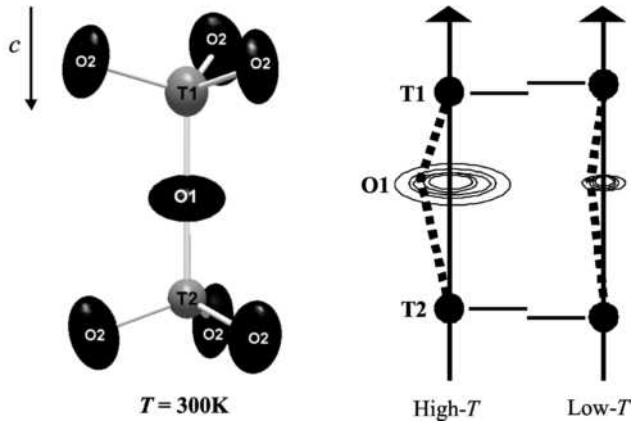

FIGURE 4. (**left**) Configuration of the anisotropic displacement ellipsoids of the framework sites in *P*31*c* kalsilite at 300 K (probability level: 99%). (**right**) Schematic view of the mechanism responsible for the structure expansion along [0001]: the decrease of libration of the O1 site at low *T* might: (1) drive the center of gravity of the electron density toward the triad axis, and (2) consequently lead to a slight increase of the intra-tetrahedral bond distance at low *T* and thus negative thermal expansion along [001].

In the absence of internal deformation of the tetrahedra, non-linear T1-O1-T2 angles can only be achieved by local tilts of the T1 and T2 tetrahedra. That the kalsilite structure has locally tilted tetrahedra is also suggested by the large values for U_{33} of the O2 oxygen atom (Table 2; Fig. 4). The same pattern of anisotropic ellipsoids was observed for the basal O atoms of the T1 and T2 tetrahedra in nepheline (Angel et al. 2008). But, unlike nepheline in which the presence of super-lattice diffraction spots indicates that the tilts are static and form an incommensurate pattern of distortion, it is not possible to determine by diffraction whether these tilts are dynamic or static within the structure of *P*31*c* kalsilite.

On cooling from room temperature to 100 K, the T1-T2 distance increases by 0.013 Å, and both the U_{11} parameter of the O1 site and the U_{33} of the O3 site in kalsilite decrease significantly (Table 2). Together, these changes indicate that the local tilts of the T1 and T2 tetrahedra are reduced on cooling. Again, one can estimate from the measured increase in the T1-T2 distance that the increase in the local value of the T1-O-T2 bond angle is of the order of 5°. The increase in the T1-T2 distances alone due to decreased tilting is sufficient to account for all of the negative thermal expansion of the [0001] direction at low temperatures (Figs. 2 and 4). A similar mechanism, whether an increase in static tilting of the tetrahedra or, more likely, increased amplitude of librational motion of the tetrahedra, is presumably responsible for the continued negative thermal expansion of this axis at higher temperatures (Hovis et al. 2003). This is completely the opposite behavior to that observed for the T1 and T2 tetrahedra in nepheline, which become more tilted at low temperatures, or the T3 and T4 tetrahedra in nepheline, which exhibit no significant change in tilts with temperature.

Only the rotations of the tetrahedra around [0001] in the average structure refinement (the tilting not being reflected in refined oxygen positions) contribute to changes in the bond lengths between the extra-framework K cation and the framework O atoms as temperature is changed. The K position is located on a triad axis at the center of the channels formed by the ditrigonal rings of the framework, approximately halfway between two consecutive (0001) sheets of tetrahedra, and approximately at the same *z*-coordinate as the O1 atoms. The coordination shell of the K-site thus consists of nine framework O atoms, with three independent groups of bond-distances (Table 3). The fractional coordinates of the K site do not change with temperature, so the small decrease of 0.007 Å in the three equivalent K-O1 bonds from 300 to 100 K is due to the overall contraction of the *a*-axis, which is a consequence of the increased rotation of the tetrahedra. The K is also bonded to three O2 atoms in each of the 6mR lying immediately above and below it (Fig. 1). The increased rotation of the T2 tetrahedra with decreasing temperature pushes the O2 atoms out into the channels and thus reduces the K-O2 distances more quickly than K-O1; between 300 and 100 K these decrease by 0.016 and 0.010 Å, respectively (Table 3).

The contrast in the structural response of nepheline and kalsilite to temperature is strong, and initially surprising given their structural homologies. This suggests that the detailed distortions of such frameworks, often governed by the extra-framework population, are important for determining the thermodynamic properties such as thermal expansion or compressibility.

While kalsilite contains a single type of 6mR with trigonal symmetry, nepheline has two distinct 6mRs with two different deformations as a result of the partial collapse of the framework to produce smaller extra-framework sites for the smaller Na cations that occupy ¾ of the channels. The more expanded of the two rings in nepheline, which might be expected to be similar to the rings in kalsilite, has trigonal symmetry, but is far less distorted than the rings in kalsilite. This channel in nepheline is comprised of T3 and T4 tetrahedra, and it forms the channel that is occupied by typically 50% K, 25% Na, and 5% Ca, with 20–25% vacancies (Gatta and Angel 2007; Angel et al. 2008). The tilts of the T3 and T4 tetrahedra in nepheline, which might have been expected to be similar to kalsilite are, instead, much greater. This can be explained in terms of the bonding environment of the apical O2 oxygen that forms the T3-O2-T4 link; it is coordinated to one "K" in the larger channel as well as to one Na in a smaller adjacent channel. Indeed, it forms one of the shortest, and presumably strongest, Na-O bonds to the latter. The T1 and T2 tetrahedra of nepheline only occur in the more distorted 6mR that form the channels for the Na atoms. The bridging O1 oxygen formally lies on a triad passing through T1-O1-T2, which would place it equidistant from three Na atoms, in the same way the O1 oxygen is surrounded by three K-sites in kalsilite. With this configuration, the Na-O distances are too long to satisfy the bonding requirements of the Na, and a significant shift of O1 off the triad axis (1/3, 2/3, *z*) to a general position (*x*, *y*, *z*), with a formal average occupancy of 1/3, occurs (e.g., Tait et al. 2003). In a natural nepheline, the T1-O1-T2 angle is ~151° at 298 K (Angel et al. 2008).

The cause of the different structural evolution between nepheline and kalsilite with temperature can now be ascribed to the different extra-framework content and, in particular, to the presence of Na because of the tetrahedral tilts it forces on the framework. In particular, the greater tetrahedral tilts in nepheline compared to kalsilite prevent the free rotation of the tetrahedra around [0001]; the changes in rotations as measured by O-O-O

angles in the 6mR on cooling to 100 K average 0.3° in nepheline (Angel et al. 2008) and are much smaller than the 2.5° change in O-O-O angles due to tetrahedral rotation in kalsilite. So, while the tetrahedral rotations provide the volume reduction in kalsilite, increased tetrahedral tilts are required to generate the volume reduction in nepheline with decreased temperature. The increased tilts also serve to improve the bonding environment of the Na atom in the channels of nepheline, with the bond to the bridging O1 oxygen showing a decrease with temperature that is 10 times that of any other Na-O bond (Angel et al. 2008).

The dominant influence of the Na content on the thermo-elastic properties of nepheline and kalsilite through its control on framework tilts is indicated by two observations. First, in volcanic kalsilite with X_{Ks} = 0.955 (Perrotta and Smith 1965) the distance from the extra-framework cation site to the O1 oxygen is only 2.76 Å, significantly shorter than the ~2.98 Å found in this study for "pure" kalsilite. In nepheline this distance is reduced to 2.56 Å for the site containing 100% Na. Second, only almost pure kalsilites [this measurement and X_{Ks} = 0.983 from Hovis et al. (2003)] exhibit negative thermal expansion along [0001], which can only occur when the tilts of the tetrahedra decrease with decreasing temperature. Kalsilites with X_{Ks} = 0.886 and X_{Ks} = 0.790 (i.e., 11.4 and 21% Na) instead exhibit positive thermal expansion, as observed for all nephelines (Hovis et al. 2003).

The comparison of the low-temperature structural evolution and thermo-elastic behavior of nepheline and kalsilite has shown that two homeotypic compounds do not necessarily respond to changes in temperature or pressure in the same way. Instead, the extra-framework population, through its bonding to the framework anions and thus the detailed deformation of the framework, can play a fundamental role in determining the structural response to temperature changes and thus the thermodynamic properties of these minerals.

ACKNOWLEDGMENTS

G.D.G. thanks the Italian CNR and the University of Milan (PUR-2008) for financial support. Measurements were performed at Virginia Tech (VT) with the support of the College of Science and NSF grant EAR-0738692 to N.L. Ross and R.J. Angel. We thank J. Zhao and C. Slebodnick for assistance with experimental measurements at VT. The associate editor Hongwu Xu and the reviewers Guy Hovis and Kimberly Tait are warmly thanked for helpful and prompt reviews.

REFERENCES CITED

Abbott Jr., R.N. (1984) $KAlSiO_4$ stuffed derivates of tridymite: Phase relationships. American Mineralogist, 69, 449–457.

Andou, Y. and Kawahara, A. (1982) The existence of high-low inversion point of kalsilite. Mineralogical Journal, 11, 72–77.

——— (1984) The refinement of the structure of synthetic kalsilite. Mineralogical Journal, 12, 153–161.

Angel, R.J., Gatta, G.D., Boffa-Ballaran, T., and Carpenter, M.A. (2008) The mechanism of coupling in the modulated structure of nepheline. Canadian Mineralogist, 46, 1465–1576

Capobianco, C.J. and Carpenter, M.A. (1989) Thermally induced changes in kalsilite. American Mineralogist, 74, 797–811.

Carpenter, M.A. and Cellai, D. (1996) Microstructures and high-temperature phase transitions in kalsilite. American Mineralogist, 81, 561–584.

Cellai, D., Bonazzi, P., and Carpenter, M.A. (1997) Natural kalsilite, $KAlSiO_4$, with *P*31*c* symmetry: Crystal structure and twinning. American Mineralogist, 82, 276–279.

Cellai, D., Gesing, T.M., Wruck, B., and Carpenter, M.A. (1999) X-ray study of the trigonal-hexagonal phase transition in metamorphic kalsilite. American Mineralogist, 84, 1950–1955.

Dollase, W.A. and Freeborn, W.P. (1977) The structure of $KAlSiO_4$ with $P6_3mc$ symmetry. American Mineralogist, 62, 336–340.

Downs, R.T. (2000) Analysis of harmonic displacement factors. In R.M. Hazen and R.T. Downs, Eds., High-Temperature and High-Pressure Crystal Chemistry, 41, p. 61–117. Reviews in Mineralogy and Geochemistry, Mineralogical Society of America and Geochemical Society, Chantilly, Virginia.

Downs, R.T., Gibbs, G.V., Bartelmehs, K.L., and Boisen Jr., M.B. (1992) Variations of bond lengths and volumes of silicate tetrahedra with temperature. American Mineralogist, 77, 751–757.

Gatta, G.D. and Angel, R.J. (2007) Elastic behavior and pressure-induced structural evolution of nepheline: Implications for the nature of the modulated superstructure. American Mineralogist, 92, 1446–1455.

Gottardi, G. (1979) Topologic symmetry and real symmetry in framework silicates. Mineralogy and Petrology, 26, 39–50.

Gregorkiewitz, M. and Schäfer, H. (1980) The structure of $KAlSiO_4$-kaliophilite-O1: Application of the subgroup-supergroup relations to the quantitative space group determination of pseudosymmetric crystals. Sixth European Crystallographic meeting, Barcelona, July 28–August 1, Abstract, p. 155.

Henderson, C.M.B. and Roux, J. (1976) The thermal expansions and crystallographic transformations of some synthetic nephelines. In G.M. Biggar, Ed., Progress in Experimental Petrology, p. 60–69. NERC Report 3, U.K.

——— (1977) Inversions in sub-potassic nephelines. Contributions to Mineralogy and Petrology, 61, 279–298.

Henderson, C.M.B. and Taylor, D. (1982) The structural behavior of the nepheline family: (1) Sr and Ba aluminates (MAl_2O_4). Mineralogical Magazine, 45, 111–127.

——— (1988) The structural behavior of the nepheline family: (3) Thermal expansion of kalsilite. Mineralogical Magazine, 52, 708–711.

Hovis, G.L. and Crelling, J.A. (2000) The effects of excess silicon on immiscibility in the nepheline-kalsilite system. American Journal of Science, 300, 238–249.

Hovis, G.L. and Roux, J. (1993) Thermodynamic mixing properties of nepheline-kalsilite crystalline solutions. American Journal of Science, 293, 1108–1127.

——— (1999) Thermodynamics of excess silicon in nepheline and kalsilite crystalline solutions. European Journal of Mineralogy, 11, 815–827.

Hovis, G.L., Crelling, J., Wattles, D., Dreibelbis, B., Dennison, A., Keohane, M., and Brennan, S. (2003) Thermal expansion of nepheline-kalsilite crystalline solutions. Mineralogical Magazine, 67, 535–546.

Hovis, G.L., Person, E., Spooner, A., and Roux, J. (2006) Thermal expansion of highly silicic nepheline–kalsilite crystalline solutions. Mineralogical Magazine, 70, 383–396.

Hovis, G.L., Mott, A., and Roux, J. (2009) Thermodynamic, phase equilibrium, and crystal chemical behavior in the nepheline-kalsilite system. American Journal of Science, 309, 397–419.

Kawahara, A., Andou, Y., Marumo, F., and Okuno, M. (1987) The crystal structure of high temperature form of kalsilite ($KAlSiO_4$) at 950 °C. Mineralogical Journal, 13, 260–270.

Klyne, W. and Prelog, V. (1960) Description of steric relationships across single bonds. Experientia, 16, 521.

Merlino, S. (1984) Feldspathoids: their average and real structures. In W.L. Brown, Ed., Feldspars and Feldspathoids. Structures, Properties, and Occurrences, 137, p. 435–470. NATO Advanced Study Institute, Series C: Mathematical and Physical Sciences, Dordrecht, Netherlands.

Oxford Diffraction (2007) CrysAlis Software system, Xcalibur CCD system. Oxford Diffraction, Abingdon, Oxfordshire.

Perrotta, A.J. and Smith, J.V. (1965) The crystal structure of kalsilite $KAlSiO_4$. Mineralogical Magazine, 35, 588–595.

Sahama, T.G. (1962a) Perthite-like exsolution in the nepheline-kalsilite system. Norsk Geologisk Tidsskrift, 43, 168–179.

——— (1962b) Order-disorder in natural nepheline solid solutions. Journal of Petrology, 3, 65–81.

Sandiford, M. and Santosh, M. (1991) A granulite facies kalsilite-leucite-hibonite association from Punalur, Southern India. Mineralogy and Petrology, 43, 225–236.

Sheldrick, G.M. (2008) A short history of SHELX. Acta Crystallographica A, 64, 112–122.

Smith, J.V. and Sahama, T.G. (1957) Order-disorder in kalsilite. American Mineralogist, 42, 287–288.

Tait, K.T., Sokolova, E., Hawthorne, F.C., and Khomyakov, A.P. (2003) The crystal chemistry of nepheline. Canadian Mineralogist, 41, 61–70.

Tuttle, O.F. and Smith, J.V. (1958) The nepheline-kalsilite system: II. Phase relations. American Journal of Science, 256, 571–589.

Wilson, A.J.C. and Prince, E. (1999) International Tables for X-ray Crystallography, Volume C: Mathematical, physical and chemical tables, 2nd edition. Kluwer Academic, Dordrecht, Netherlands.

Xu, H. and Veblen, D.R. (1996) Superstructures and domain structures in natural and synthetic kalsilite. American Mineralogist, 81, 1360–1370.

MANUSCRIPT RECEIVED DECEMBER 15, 2009
MANUSCRIPT ACCEPTED FEBRUARY 10, 2010
MANUSCRIPT HANDLED BY HONGWU XU